MiR30a Inhibits Inflammation by Targeting Klf14 in Autoimmune Hepatitis

Xiaofeng Yuan (yuanxf5@mail.sysu.edu.cn)
The Third Affiliated Hospital of Sun Yat-Sen University LingNan Hospital

Shunwen Pan
The Third Affiliated Hospital of Sun Yat-Sen University

Mingliang Li
The Third Affiliated Hospital of Sun Yat-Sen University LingNan Hospital

Li Quan
The Third Affiliated Hospital of Sun Yat-Sen University

Kouxing Zhang
The Third Affiliated Hospital of Sun Yat-Sen University

Xiaogang Bi
The Third Affiliated Hospital of Sun Yat-Sen University LingNan Hospital

Research Article

Keywords: miR30a, inflammation, Klf14, autoimmune hepatitis, liver inflammatory injury

Posted Date: September 23rd, 2021

DOI: https://doi.org/10.21203/rs.3.rs-917370/v1

Abstract

MiR30a plays diverse roles in inflammatory diseases, including autoimmune hepatitis (AIH). Klf14 is associated with the inflammation in AIH. We investigated whether miR30a exerts its regulatory function via Klf14. Concanavalin A (Con A)-induced AIH mice were infected with a miR30a agomir or antagomir. MiR30a expression was quantified using qRT-PCR. TargetScan and luciferase reporter assays were used to predict the relationship between miR30a and Klf14. Liver inflammation was evaluated by measuring serum alanine transaminase (ALT) and aspartate aminotransferase (AST) levels, performing histology, and measuring mRNA expressions of inflammatory cytokines and Klf14 by qRT-PCR, protein of Klf14 by western blotting, and Tregs by FACS. MiR30a was downregulated in the hepatocytes (HCs) of AIH mice, which was negatively associated with the liver inflammation. MiR30a overexpression alleviated the inflammation, whereas downregulation of endogenous miR30a aggravated it. The mRNA and protein level of Klf14 were inversely correlated with the miR30a expression. The luciferase reporter assay validated the relationship between Klf14 and miR30a. Moreover, the frequency of Tregs was consistently correlated with the expression of miR30a. MiR30a may play an essential role in AIH, and its ability to regulate the inflammatory responses may, at least partially, be mediated by targeting Klf14 to modulate Tregs.

Introduction

Autoimmune hepatitis (AIH) is a chronic disorder that can present acutely and is characterized by hepatocellular necrosis and inflammation [1]. The specific mechanism underlying AIH remains unclear. Concanavalin A (Con A)-induced hepatitis is a well-established animal model of AIH that has been used in numerous preclinical studies of AIH pathogenesis [2,3]. Accumulating evidence has demonstrated that miR30 plays diverse roles in inflammation [4]. In regards to liver diseases, decreased expression of miR30 in hepatocytes (HCs) of the fibrotic liver and upregulation of miR30 could prevent liver fibrosis and inflammation [5,6]. Based on our observation of the decreased expression of miR30a in AIH mice, we further investigated the roles of miR30a and its pathways involved in AIH.

Moreover, Krüppel-like factors (Klfs) regulate the pathogeneses of many diseases, including inflammatory disorders. Previous studies have reported the regulatory functions of Klf14 in liver diseases [7-9]. One previous study showed that Klf14 played a certain role in AIH by modulating regulatory T cells (Tregs) [10]. Impairment of Tregs is key to the development of AIH [11,12]. Coincidentally, Klf14 is also a potential target of miR30a. Thus, we investigated whether overexpression of miR30a could serve as a therapeutic tool to inhibit liver inflammation by modulating Klf14 expression to regulate Tregs frequency in a Con A-induced AIH mouse model.

Results

Establishment of an AIH model and endogenous miR30a expression in AIH mice

Successful establishment of AIH in mice is verified in Fig. 1A-C. After administration of Con A, serum ALT and AST levels increased significantly as compared to those in the control group (Fig. 1A). Fig. 1B shows H&E staining of the liver in both the control (Ctr) group and Con A-induced (Con A) group. We observed significant disruptions in liver structure and lymphocyte infiltration in the liver of the Con A group. Furthermore, we detected higher mRNA expression of proinflammatory cytokines (CD68, TNF-α, IL-1β, and IL-6) by qRT-PCR in the Con A group (Fig. 1C). The effect of Con A on hepatic inflammatory injury was consistent with previous findings.

To evaluate whether miR30a was aberrantly expressed in the HCs of AIH mice, the expression of miR30a was determined. MiR30a expression was significantly downregulated in the HCs of Con A-induced AIH mice. Fold changes in miR30a expression were detected using qRT-PCR and presented as ratios to U6B and RNU44 expression (Fig. 1D). The results showed that miR30a expression in the HCs of AIH mice was significantly lower than that in the control mice, indicating that inflammation suppressed endogenous miR30a expression in AIH.

Overexpression and downregulation of miR30a regulated hepatic inflammation in AIH

We established the overexpression and downregulation of miR30a in AIH mice. After pretreatment with miR30a agomir followed by Con A induction, we performed qRT-PCR to confirm the overexpression of miR30a. As shown in Fig. 2A, the miR30a agomir increased the expression of miR30a to a substantially high level (Con A vs. agomir + Con A, ***p <0.001), whereas the miR30a agomir negative control group showed a similar miR30a expression level (Con A vs. agomir NC + Con A, not significant [NS]). We then established the blockage of endogenous miR30a expression in the HCs of AIH mice. After transfecting miR30a antagomir followed by Con A induction, the miR30a expression level dramatically decreased compared with that of control group (Con A vs. antagomir + Con A, **p <0.01), whereas the negative control group showed similar miR30a expression levels (Con A vs. antagomir NC + Con A, NS). These data confirmed that HCs were successfully modulated with miR30a agomir and antagomir.

We then tested the influence of overexpression or downregulation of miR30a on hepatic inflammation in the AIH model. As shown in Fig. 2B, serum levels of ALT and AST were measured in the different groups. ALT and AST decreased back to a significantly low level in the agomir + Con A group (Con A vs. agomir + Con A, ****p < 0.0001), whereas they rose even higher when the endogenous expression of miR30a was further suppressed in the antagomir + Con A group (Con A vs. antagomir + Con A, **p < 0.01, *p < 0.05). In addition, the mRNA levels of proinflammatory cytokines (CD68, TNF-α, IL-1β, and IL-6) were significantly decreased in the miR30a agomir + Con A group, whereas they increased back to a high level in the miR30a antagomir + Con A group (Fig. 2C). The hepatic inflammation caused by Con A and the effects of

miR30a agomir or antagomir treatment were further confirmed by the liver histology results (Fig. 2D). These data suggest that overexpression of miR30a could alleviate HCs inflammation, whereas downregulation of endogenous miR30a expression aggravated HCs inflammation in AIH mice.

The interaction between miR30a and Klf14 in AIH

TargetScan 7.0 predicted Klf14 to be a target of miR30a. Therefore, we tested the mRNA and protein levels of Klf14 in the HCs of AIH mice transfected with miR30a agomir or antagomir. The results in Fig. 3A show that Con A induction caused a significant increase in the expression of Klf14 mRNA (Ctr vs. Con A, **p <0.01). However, Klf14 expression significantly decreased back to a low level in miR30a overexpressing HCs (Con A vs. agomir + Con A, ***p < 0.001), whereas it was upregulated in the miR30a downregulated HCs (Con A vs. antagomir + Con A, *p <0.05). Similar results were also observed for Klf14 protein levels (Fig. 3B). The expression of miR30a was inversely correlated with Klf14 expression, indicating that miR30a might regulate inflammation in AIH by targeting Klf14. To validate this assumption, a luciferase reporter assay was performed to confirm the relationship between Klf14 and miR30a. The putative miR30a binding site in the 3'-UTR of Klf14 gene is shown in Fig. 3C, and D. The results showed that miR30a agomir significantly decreased the luciferase activity of Klf14 3'-UTR, but had little effect on the Klf14 3'-UTR mutant, which confirmed that Klf14 was a target of miR30a, and that miR30a expression was negatively correlated with Klf14 expression.

MiR30a regulates HCs inflammation by targeting Klf14 to modulate Tregs frequency

In order to examine the interactions among miR30a, Klf14 and Tregs, we sought to explore the changes in the frequency of Tregs in different groups by FACS. As shown in Fig. 4, after the administration of Con A, we observed a significantly decreased frequency of Tregs in liver MNCs (Ctr vs. Con A, ***p < 0.001). After overexpression of miR30a by agomir, frequency of Tregs increased back to a substantially high level (Con A vs. agomir + Con A, ***p < 0.001), with mRNA and protein levels of Klf14 decreasing back (see the above mentioned Fig. 3A, B). Conversely, in miR30a-downregulated AIH mice, reduced Tregs frequency (Con A vs. antagomir + Con A, *p < 0.05) was accompanied by increased Klf14 expression (see the above mentioned Fig. 3A, B). These results indicate that miR30a exerts its anti-inflammatory effect by targeting Klf14 to modulate Tregs in AIH.

Discussion

This study showed that the expression of miR30a was inhibited by inflammation in AIH mice, accompanied by changes in Klf14 expression and Tregs frequency. MiR30a plays an essential role in liver injury in AIH. Upon further regulation of miR30a expression in AIH mice by miR30a agomir and antagomir, expected trends were found in the changes in Klf14 expression and Tregs frequency. Interestingly, Klf14

was predicted and confirmed to be a direct target of miR30a. These results suggest that miR30a may play an essential role in the regulation of the inflammatory responses in AIH, at least in part, via Klf14 regulation of Tregs.

One previous study has already shown that Klf14 knockout (KO) could promote the differentiation of CD4 + cells to adaptive Tregs more readily and enhanced Tregs suppressor function both *in vitro* and *in vivo* via chromatin remodeling at the FOXP3 TSDR. In addition, KLF14 KO mice were resistant to experimentally induced colitis [13]. These results indicate that Klf14 serves as an important regulator of Tregs differentiation and biological function. In our study, we also observed an elevated Klf14 level and decreased Tregs frequency in AIH mice; meanwhile, when the Klf14 expression was downregulated by miR30a agomir, the ratio of Tregs was significantly rescued, which was consistent with the above study. However, another study concluded that transfection of Klf14 by recombinant adenoviral vector protected the liver by increasing the frequency of Tregs in AIH mice [10]. These contradictory findings require further investigation. More importantly, the underlying molecular mechanism by which Klf4 in HCs influences the frequency of Tregs remains to be elucidated.

Several previous studies have shown that miR30a is aberrantly expressed in diverse diseases [14–18]. MiR30a is widely known as a tumor suppressor that participates in tumorigenesis [19–22]. Although the role of miR30a in tumors has been well established, its role in AIH warrants further study. Geng et al. found that the herbal extract thymoquinone exerted an anti-fibrotic effect by upregulating miR30a expression, indicating the anti-fibrotic potential of miR30a in the liver [23]. Here, we aimed to explore the anti-liver inflammation potential of miR30a transfection in AIH, which is considered to be a liver disease relevant to autoimmunity and inflammation. We found that inflammation inhibited miR30a expression in AIH mice, and overexpression or downregulation of miR30a could influence the inflammatory responses. These effects of miR30a were accompanied by the expected changes in Klf14 expression and Tregs frequency. Based on these results, we inferred that miR30a might exert its protective effects on AIH by targeting Klf14 and increasing the number of Tregs. Together, our findings provide new insights into the mechanisms of AIH and indicate that miR30a is an effective therapeutic target for AIH or other Tregs-related liver diseases.

Notably, miR30a does not always play a protective role against diseases, indicating that this role may be disease-specific. A meta-analysis showed that an increase in miR30a expression was associated with a high incidence of contrast-induced nephropathy [24]. A recent study by Wang et al. showed that miR30a is associated with blood–brain barrier damage in acute cerebral ischemia [25]. The above evidence reminds us to pay attention to miR30a-related pathogenesis of different diseases. Both contrast-induced nephropathy and acute cerebral ischemia are ischemia diseases [26,27]. In contrast, AIH is closely related to inflamation and immune-mediated liver injury, and miR30a plays a protective role against inflammation and immune-mediated liver injury, as shown in our present study. Therefore, it is reasonable to assume that miR30a may represent as an ideal target for the the treatment of inflammation and immune-mediated liver diseases.

As was shown in our analysis using TargetScan, miR30a can regulate hundreds of downstream genes in mice. This raises the question: are there any other downstream genes and pathways that are regulated by miR30a in AIH? Further, is there any discrepancy in the function of miR30a among species, as we only employed an AIH mouse model in the present study? The mechanisms of action of miR30a in AIH may be complicated. Further studies are needed to tailor miRNA function to achieve the desired therapeutic effect in a specific disease.

Conclusions

Herein, we employed an AIH model to examine the potential of miR30a as a therapeutic tool to eliminate liver inflammation by modulating Klf14 to regulate Tregs. In conclusion, our data show that miR30a might exert its protective effect by regulating the downstream Klf14 gene, leading to the changed pattern of Tregs in AIH mice.

Materials And Methods

AIH animal model and miRNA transfection

Eight-week-old male C57BL/6 mice were obtained from Vital River (Beijing, China). AIH in mice was induced by intravenous injection of a single dose of freshly prepared Con A (15 mg/kg, Sigma-Aldrich Chemical Co., China). After Con A administration, blood samples were collected for measurement of plasma alanine transaminase (ALT) and aspartate aminotransferase (AST) levels using mouse AST ELISA kits (Biotron Diagnostics, Hemet, CA, USA), according to the manufacturer's instructions. MiR30a expression is regulated *in vivo* by miR30a agomir or antagomir. MiR30a agomir, antagomir, or their negative controls (all form RiboBio, Guangzhou, China) were injected via the tail vein in mice 72 h before Con A administration (n = 5 animals per group).

All experimental animal protocols followed the regulations for the Administration of Affairs Concerning Experimental Animals (AdminReg, China) and were approved by the Ethics Committee of Animal Experiments and monitored by the Department of Experimental Animals of the Third Affiliated Hospital of Sun Yat-Sen University LingNan Hospital. All the authors confirmed that the experiments complied with the ARRIVE guidelines.

TargetScan and luciferase reporter assay

TargetScan 7.0 was used to predict the target genes interacting with miR30a. A list of candidate miR30a targets was obtained. Among them, Klf14 appeared to be a promising target, as it was implicated in the pathology of inflammation in the liver.

To confirm the relationship between miR30a and Klf14, fragments of the 3'-UTR (Wt) containing the binding site of miR30a, or a 3'-UTR mutant (Mut) of Klf14 were cloned into pMIRREPORTTM luciferase

vectors (Huayueyang, Beijing, China). HCs were co-transfected with the luciferase reporter vector, Renilla luciferase control vector (pRL-hTK), and the miR30a agomir or negative control using LipofectamineTM 2000 (Invitrogen, Carlsbad, CA, USA). Luciferase assays were performed 48 h after transfection using the dual-luciferase reporter assay system (Promega, San Luis Obispo, CA, USA) according to the manufacturer's protocol. Firefly luciferase activity was normalized to Renilla luciferase activity.

Cell isolation and culture

Primary mouse HCs and liver mononuclear cells (MNCs) were isolated as previously described [11]. Briefly, mouse livers were perfused with liberase TM solution (Sigma-Aldrich, St. Louis, MO, USA) after euthanasia, filtered through a 70 μm nylon cell strainer (BD Falcon, Franklin Lakes, NJ, USA), and centrifuged at 20× g for 5 min. The pellets were suspended and placed on the surface of 30% Percoll solution, centrifuged at 1000 × g for 10 min at 4 °C and washed once with phosphate-buffered saline (PBS). HCs were used for mRNA/miRNA isolation or protein extraction. Supernatants containing MNCs were collected, resuspended in 30% Percoll, and gently overlaid onto 70% Percoll. After centrifugation at 1000 × g for 30 min, liver MNCs were harvested from the interphase, washed twice with PBS, and then resuspended for further fluorescence-activated cell sorting (FACS) analysis.

RNA isolation and quantitative reverse transcription-polymerase chain reaction

Total miRNAs from HCs were isolated using the mirVana™ miRNA isolation kit (Ambion, Austin, TX, USA) following the manufacturer's instructions. RNA was isolated from liver tissue after exosome treatment using TRIzol reagent (Life Technologies, MD, USA) and digested with DNase I (Fermentas, Glen Burnie, MD, USA) according to the manufacturer's protocol. Subsequently, total RNA was reverse-transcribed to cDNA using a RevertAid First Stand cDNA Kit (Thermo Fisher Scientific, Rutherford, NJ, USA). The expression levels of miR30a, Klf14, and inflammatory cytokines were quantified by quantitative reverse transcription-polymerase chain reaction (qRT-PCR) using a 7500 Fast Real-Time PCR System (Applied Biosystems, Frederick, MD, USA) and were normalized to the expression of RNU6B (U6B), RNU44, or GAPDH. All samples were prepared and analyzed three times individually. The PCR primers used for the genes of interest are listed in Supplementary Table S1 online.

Western blotting

Total protein was extracted from HCs using Radioimmunoprecipitation buffer. Western blot analysis was performed as previously described [28]. Proteins were loaded into gels, subjected to sodium dodecyl sulfate-polyacrylamide gel electrophoresis and transferred to polyvinylidene difluoride membranes. The membranes were incubated with anti-Klf14 polyclonal antibody (rabbit anti-mouse, 1:1000, PA5-23784, Invitrogen, Carlsbad, CA, USA), anti-β-actin Polyclonal Antibody (Rabbit anti mouse, 1:4000, #4967,

CST, Beverly, MA, USA) with gentle agitation overnight at 4 ˚C. The membranes were washed three times for 5 min each with TBST (containing 0.1% Tween-20) and incubated with horseradish-peroxidase-conjugated anti-Rabbit IgG (Invitrogen) followed by chemiluminescence detection using Pierce^{TM} ECL western blotting substrate (Thermo Fisher Scientific, Rutherford, NJ, USA) according to the manufacturer's protocol. The membranes were subsequently analyzed using "Quantity One" software (Bio-Rad Laboratories, Hercules, CA, USA).

Histopathology

After sacrifice, the livers of individual mice were perfused with ice-cold PBS to remove blood components. Livers were cut into 2 × 4 × 4 mm^3 sections, fixed in 4% paraformldehyde, and embedded in paraffin. Subsequently, 5 μm slices were then cut at various depths in the tissue sections, stained with hematoxylin-eosin (H&E) and examined under light microscopy to determine the level of inflammation.

Flow cytometric analysis

Flow cytometry was conducted using a BD FACScalibur device (BD Biosciences, USA) and analyzed with FCS express V3. After washing with Hank's buffer devoid of Ca^{2+} and Mg^{2+}, 5 × 10^5 liver MNCs were blocked using in 1% bovine serum albumin at 4 °C for 30 min. Unfractionated cells were stained with allophycocyanin-conjugated anti-CD4 and PE-conjugated anti-CD25 (eBioscience, San Diego, CA, USA) monoclonal antibodies. Cells were incubated at 4 °C in the dark for 30 min, washed with PBS/1% fetal bovine serum, resuspended, and analyzed by flow cytometry using a Becton Dickinson fluorescent activated cell sorter (FACSCantoII, Becton Dickinson Immunocytochemistry Systems, San Jose, CA, USA). FACS-Diva software was used for analysis. A minimum of 2 × 10^4 gated events was acquired for each sample.

Statistical analysis

SPSS software (version 20.0) was used for all statistical analyses. Data are expressed as the mean ± standard error. All results presented represent data collected from at least three independent experiments. Results were analyzed by using the Student's t-test. Statistical significance was set at $p < 0.05$.

Abbreviations

AIH, autoimmune hepatitis; Con A, Concanavalin A; qRT-PCR, quantitative reverse transcription-polymerase chain reaction; ALT, alanine transaminase; AST, aspartate aminotransferase; FACS, fluorescence-activated cell sorting; HCs, hepatocytes; MNCs, mononuclear cells; miRNAs, microRNAs; Klfs, Krüppel-like factors; Tregs, regulatory T cells; PBS, phosphate-buffered saline; U6B, RNU6B; H&E, hematoxylin-eosin; Ctr, control; NS, not significant; KO, knockout.

Declarations

Data Availability Statement

The datasets used and/or analyzed during the current study are available from the corresponding author on reasonable request.

Author contributions

X Yuan made substantial contributions to conception and design, or acquisition of data, or analysis and interpretation of data. S Pan and M Li had been involved in drafting the manuscript or revising it critically for important intellectual content. K Zhang agreed to be accountable for all aspects of the work in ensuring that questions related to the accuracy or integrity of any part of the work were appropriately investigated and resolved. X Bi had given final approval of the version to be published. All authors read and approved the final manuscript.

Competing interests

The authors declare no competing interests.

References

1. Ahmed, A., Ali, H., Galan, M., Jiang, J. G. & Lingiah, V. Concurrent Langerhans Cell Histiocytosis and Autoimmune Hepatitis: A Case and Review of the Literature. *Cureus*, **12**, e11808 https://doi.org/10.7759/cureus.11808 (2020).
2. Yuksel, M. *et al.* Hepatitis mouse models: from acute-to-chronic autoimmune hepatitis. *Int J Exp Pathol*, **95**, 309–320 https://doi.org/10.1111/iep.12090 (2014).
3. Heymann, F., Hamesch, K., Weiskirchen, R. & Tacke, F. The concanavalin A model of acute hepatitis in mice. *Lab Anim*, **49**, 12–20 https://doi.org/10.1177/0023677215572841 (2015).
4. Caserta, S. *et al.* Severity of Systemic Inflammatory Response Syndrome Affects the Blood Levels of Circulating Inflammatory-Relevant MicroRNAs. *Front Immunol* **8**, 1977, doi:10.3389/fimmu.2017.01977 (2017).
5. Tu, X. *et al.* MicroRNA-30 Protects Against Carbon Tetrachloride-induced Liver Fibrosis by Attenuating Transforming Growth Factor Beta Signaling in Hepatic Stellate Cells. *Toxicol Sci*, **146**, 157–169 https://doi.org/10.1093/toxsci/kfv081 (2015).
6. Tu, X. *et al.* TGF-beta-induced hepatocyte lincRNA-p21 contributes to liver fibrosis in mice. *Sci Rep*, **7**, 2957 https://doi.org/10.1038/s41598-017-03175-0 (2017).
7. Pape, S., Schramm, C. & Gevers, T. J. Clinical management of autoimmune hepatitis. *United European Gastroenterol J*, **7**, 1156–1163 https://doi.org/10.1177/2050640619872408 (2019).

8. de Assuncao, T. M. *et al.* New role for Kruppel-like factor 14 as a transcriptional activator involved in the generation of signaling lipids. *J Biol Chem*, **289**, 15798–15809 https://doi.org/10.1074/jbc.M113.544346 (2014).
9. Kim, C. K., He, P., Bialkowska, A. B. & Yang, V. W. SP and KLF Transcription Factors in Digestive Physiology and Diseases., **152**, 1845–1875 https://doi.org/10.1053/j.gastro.2017.03.035 (2017).
10. Chen, X. *et al.* Overexpression of KLF14 protects against immune-mediated hepatic injury in mice. *Lab Invest*, **99**, 37–47 https://doi.org/10.1038/s41374-018-0134-4 (2019).
11. Longhi, M. S. *et al.* Vigorous activation of monocytes in juvenile autoimmune liver disease escapes the control of regulatory T-cells., **50**, 130–142 https://doi.org/10.1002/hep.22914 (2009).
12. Liberal, R. *et al.* The impaired immune regulation of autoimmune hepatitis is linked to a defective galectin-9/tim-3 pathway., **56**, 677–686 https://doi.org/10.1002/hep.25682 (2012).
13. Sarmento, O. F. *et al.* A novel role for KLF14 in T regulatory cell differentiation. *Cell Mol Gastroenterol Hepatol* **1**, 188–202 e184, doi:10.1016/j.jcmgh.2014.12.007 (2015).
14. Hayes, C. N. & Chayama, K. MicroRNAs as Biomarkers for Liver Disease and Hepatocellular Carcinoma. *Int J Mol Sci*, **17**, 280 https://doi.org/10.3390/ijms17030280 (2016).
15. Croce, C. M. & Calin, G. A. miRNAs, cancer, and stem cell division., **122**, 6–7 https://doi.org/10.1016/j.cell.2005.06.036 (2005).
16. Schueller, F. *et al.* The Role of miRNAs in the Pathophysiology of Liver Diseases and Toxicity. *Int J Mol Sci*, **19**, https://doi.org/10.3390/ijms19010261 (2018).
17. Enache, L. S. *et al.* Circulating RNA molecules as biomarkers in liver disease. *Int J Mol Sci*, **15**, 17644–17666 https://doi.org/10.3390/ijms151017644 (2014).
18. Musaddaq, G., Shahzad, N., Ashraf, M. A. & Arshad, M. I. Circulating liver-specific microRNAs as noninvasive diagnostic biomarkers of hepatic diseases in human., **24**, 103–109 https://doi.org/10.1080/1354750X.2018.1528631 (2019).
19. Paul, R., Bharambe, H. & Shirsat, N. V. Autophagy inhibition impairs the invasion potential of medulloblastoma cells. *Mol Biol Rep*, **47**, 5673–5680 https://doi.org/10.1007/s11033-020-05603-3 (2020).
20. Singh, S. V. *et al.* Restoration of miR-30a expression inhibits growth, tumorigenicity of medulloblastoma cells accompanied by autophagy inhibition. *Biochem Biophys Res Commun*, **491**, 946–952 https://doi.org/10.1016/j.bbrc.2017.07.140 (2017).
21. Kulkarni, B. *et al.* Exosome-mediated delivery of miR-30a sensitize cisplatin-resistant variant of oral squamous carcinoma cells via modulating Beclin1 and Bcl2. *Oncotarget* **11**, 1832–1845, doi:10.18632/oncotarget.27557 (2020).
22. Min, J. *et al.* microRNA-30a arbitrates intestinal-type early gastric carcinogenesis by directly targeting ITGA2., **23**, 600–613 https://doi.org/10.1007/s10120-020-01052-w (2020).
23. Geng, W., Li, C., Zhan, Y., Zhang, R. & Zheng, J. Thymoquinone alleviates liver fibrosis via miR-30a-mediated epithelial-mesenchymal transition. *J Cell Physiol*, https://doi.org/10.1002/jcp.30097

(2020).

24. Toruan, M. P. L., Pranata, R., Setianto, B. Y. & Haryana, S. M. The Role of MicroRNA in Contrast-Induced Nephropathy: A Scoping Review and Meta-Analysis. Biomed Res Int 2020, 4189621, doi:10.1155/2020/4189621 (2020).
25. Wang, P. *et al.* MicroRNA-30a regulates acute cerebral ischemia-induced blood-brain barrier damage through ZnT4/zinc pathway. *J Cereb Blood Flow Metab*, **41**, 641–655 https://doi.org/10.1177/0271678X20926787 (2021).
26. Persson, P. B., Hansell, P. & Liss, P. Pathophysiology of contrast medium-induced nephropathy. *Kidney Int*, **68**, 14–22 https://doi.org/10.1111/j.1523-1755.2005.00377.x (2005).
27. Sarvari, S., Moakedi, F., Hone, E., Simpkins, J. W. & Ren, X. Mechanisms in blood-brain barrier opening and metabolism-challenged cerebrovascular ischemia with emphasis on ischemic stroke. *Metab Brain Dis*, **35**, 851–868 https://doi.org/10.1007/s11011-020-00573-8 (2020).
28. Fan, W. *et al.* Shear-sensitive microRNA-34a modulates flow-dependent regulation of endothelial inflammation. *J Cell Sci*, **128**, 70–80 https://doi.org/10.1242/jcs.154252 (2015).

Figures

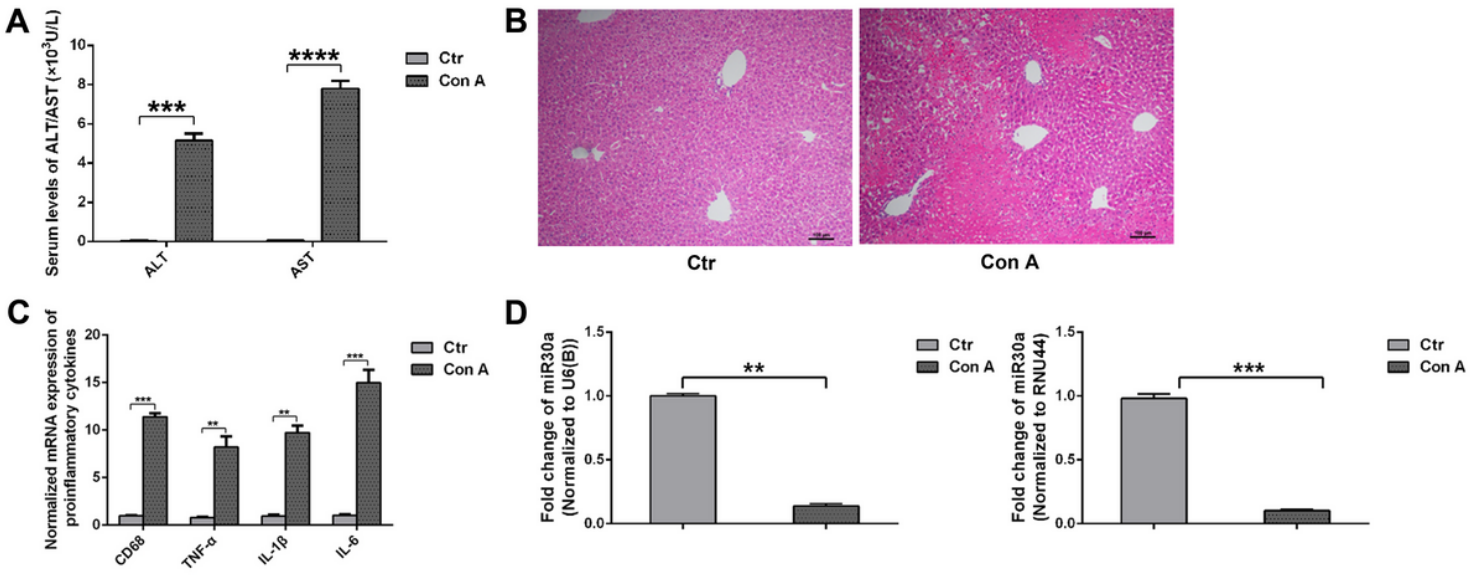

Figure 1

Establishment of a mouse autoimmune hepatitis (AIH) model and endogenous miR30a expression in AIH mice. A. Serum levels of alanine transaminase (ALT) and aspartate aminotransferase (AST) were measured. Results are shown as mean ± SD (***p <0.001, ****p < 0.0001). B. Liver tissue was stained with hematoxylin and eosin (H&E). Significant disruptions of liver structure and lymphocyte infiltration in the liver were observed in the Con A group. C. mRNA levels of proinflammatory cytokines (CD68, TNF-α, IL-1β, and IL-6) increased significantly after Con A induction (**p < 0.01, ***p <0.001). D. Fold changes in

miR30a expression as ratios to U6B (A) or RNU44 (B) expression were detected (**p < 0.01, ***p <0.001). (Ctr group: control group; Con A group: Con A-induced group)

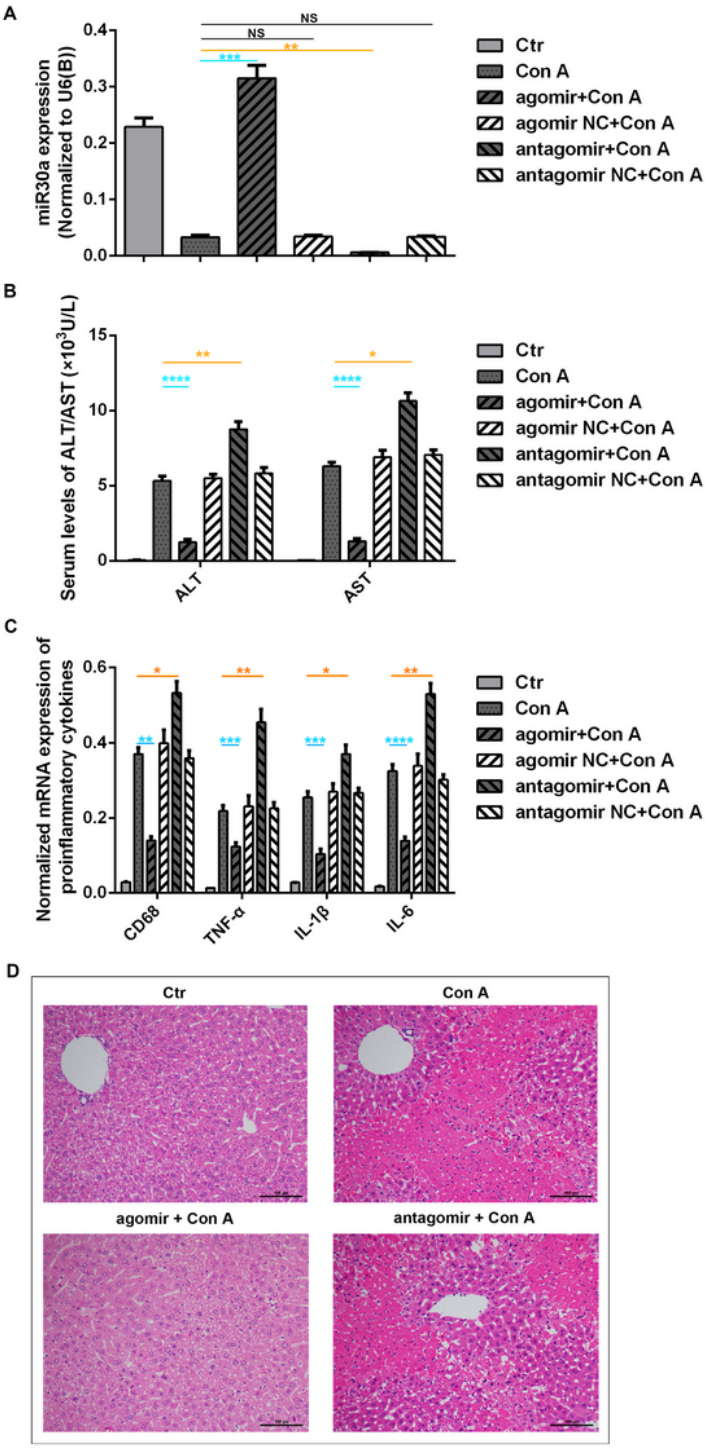

Figure 2

Effects of miR30a on the inflammation of HCs in AIH mice. Cells were transfected with miR30a agomir/antagomir and their negative controls followed by Con A induction. A. MiR30a mRNA levels as ratios to U6B levels were assessed. (Con A vs. agomir + Con A, ***p < 0.001; Con A vs. antagomir + Con A,

**p < 0.01). B. Serum levels of ALT and AST decreased back to a significantly lower level after miR30a agomir transfection (Con A vs. agomir + Con A, ****p < 0.0001). However, they increased when the endogenous expression of miR30a was further suppressed after miR30a antagomir transfection (Con A vs. antagomir + Con A, **p < 0.01, *p < 0.05). C. The mRNA expression of proinflammatory cytokines (CD68, TNF-α, IL-1β, and IL-6) decreased after miR30a agomir transfection, but increased higher after miR30a antagomir transfection (*p < 0.05, **p < 0.01, ***p < 0.001, ****p < 0.0001). D. Immunohistochemical results confirmed the inflammatory injury caused by Con A and the effects of miR30a agomir/antagomir.

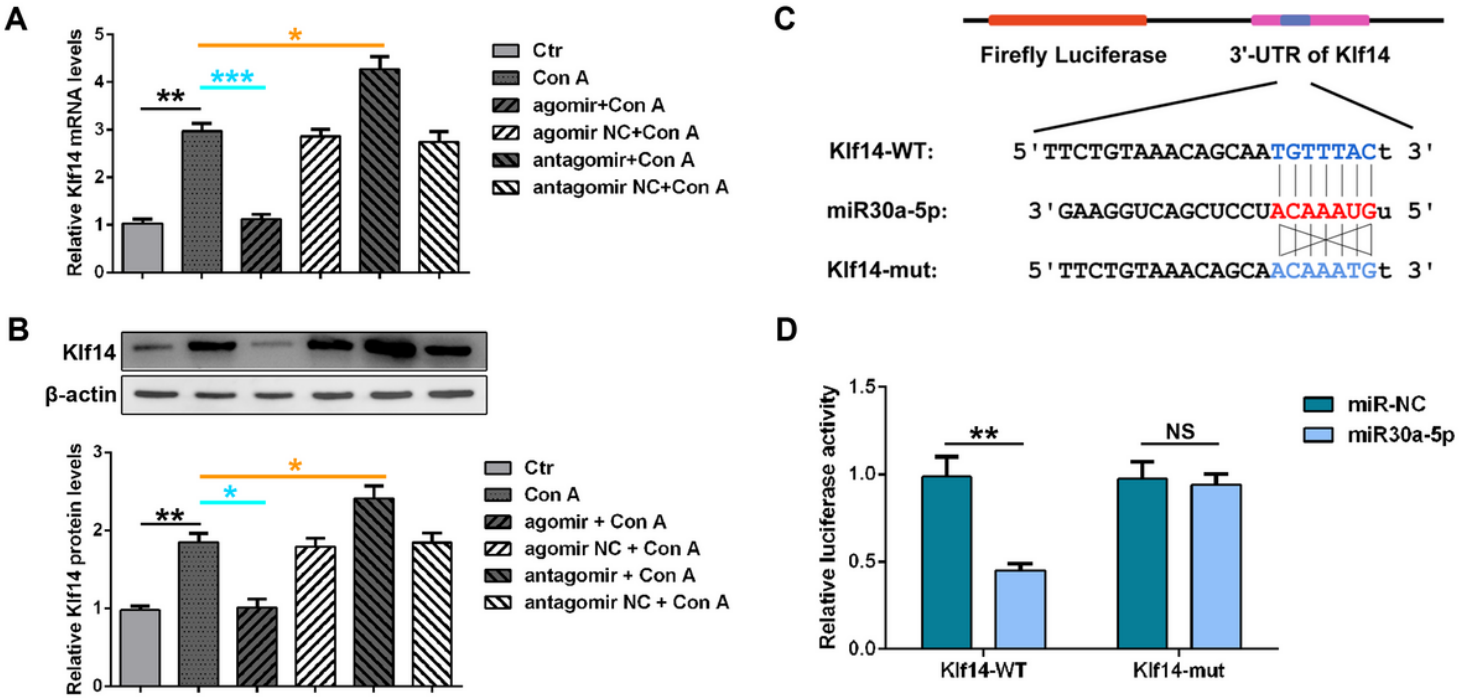

Figure 3

Analysis of the interaction between miR30a and Klf14 in HCs. A. Klf14 mRNA expression significantly increased after Con A induction (Ctr vs. Con A, **p < 0.01) but decreased in the miR30a overexpressing HCs (Con A vs. agomir + Con A, ***p <0.001), whereas it rose even higher in the endogenous miR30a-downregulated HCs (Con A vs. antagomir + Con A, *p < 0.05). B. Klf14 protein level was upregulated after Con A induction (Ctr vs. Con A, **p < 0.01). It was deficiently expressed after miR30a agomir transfection (Con A vs. agomir + Con A, *p < 0.05) but abundantly expressed in the antagomir + Con A group after miR30a antagomir transfection (Con A vs. antagomir + Con A, *p < 0.05). C, D. Luciferase reporter assay showed miR30a agomir significantly decreased the luciferase activity of Klf14 3'-UTR (**p < 0.01) but had little effect on Klf14 3'-UTR mutant (NS).

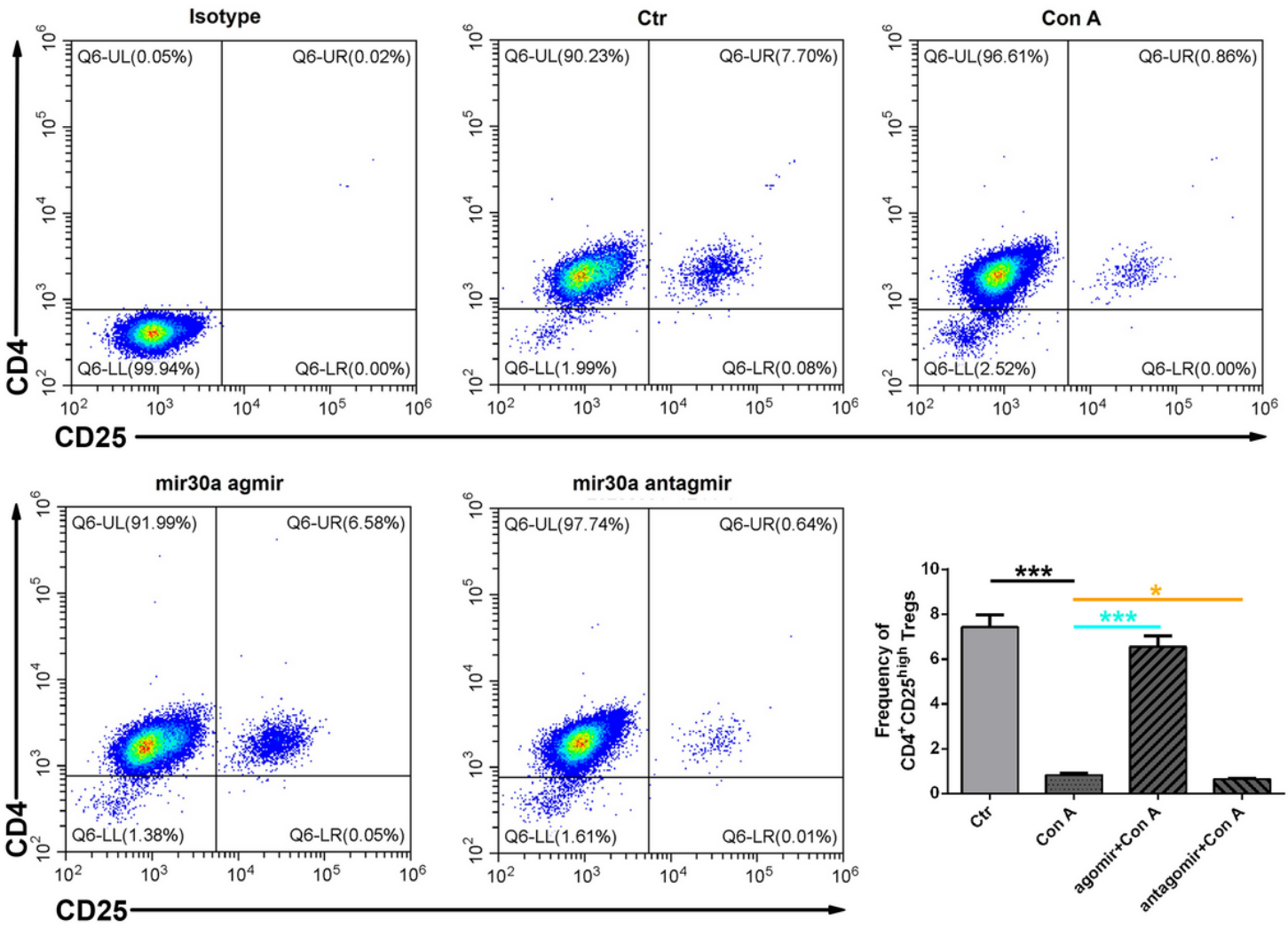

Figure 4

FACS analysis of regulatory T cells (Tregs). Con A administration induced a significant reduction in Tregs frequency in liver mononuclear cells (MNCs) (Ctr vs. Con A, ***p<0.001). A signifcant increase in the number of Tregs in liver MNCs was observed after miR30a agomir transfection (Con A vs. agomir + Con A, ***p < 0.001), whereas an even greater reduction in the number of Tregs was observed after miR30a antagomir transfection (Con A vs. antagomir + Con A, *p < 0.05).

Supplementary Files

This is a list of supplementary files associated with this preprint. Click to download.

- SupplementaryTableS1.pdf